Moriwaki and Goshima, http://dx.doi.org/10.1083/jcb.201604118

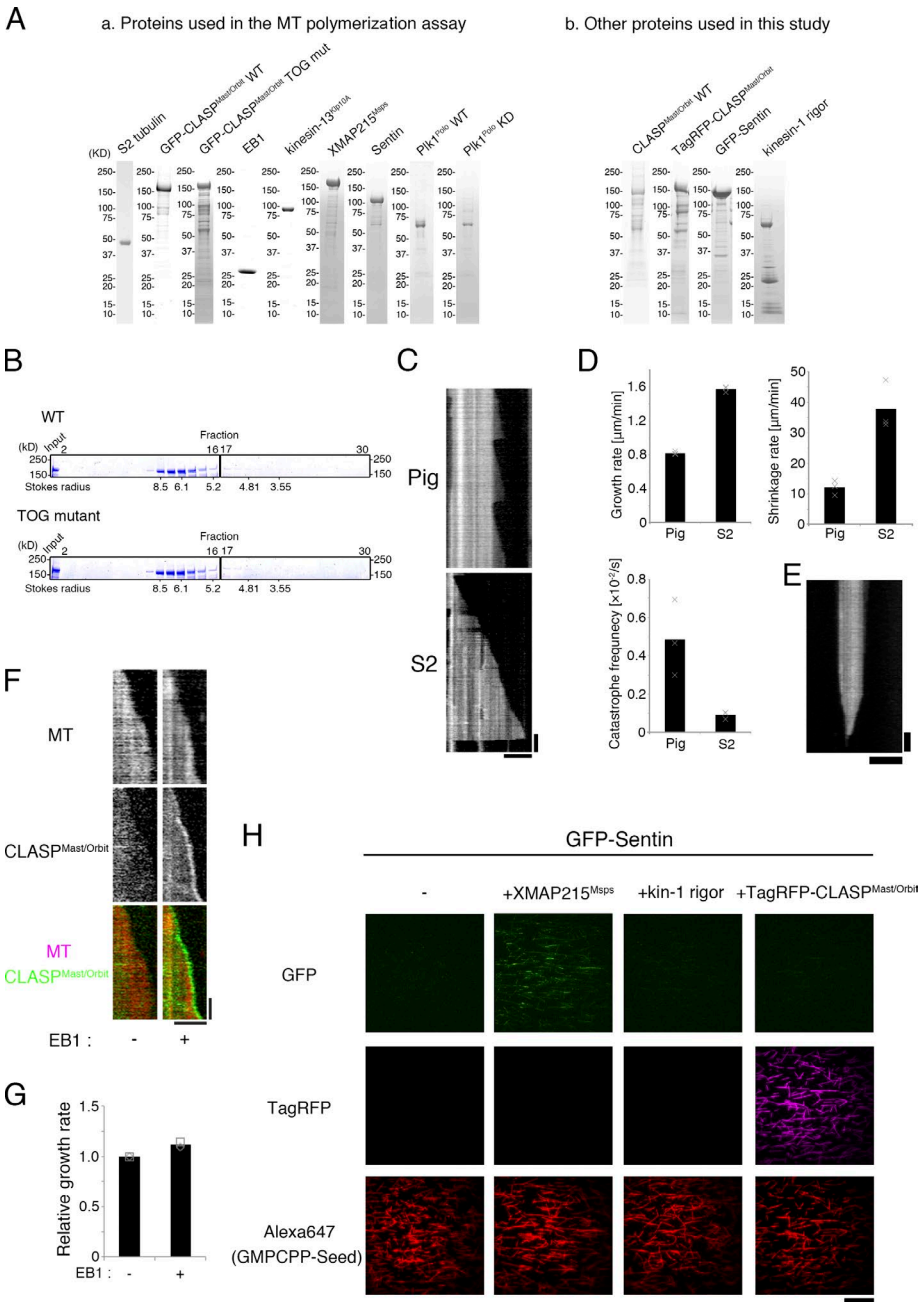

Figure S1. **Recombinant proteins used in this study, kinesin-13^{Klp10A} activity, and comparison between S2-derived tubulin and pig brain tubulin.** (A) Coomassie staining of recombinant proteins used in this study. (B) Gel filtration chromatography of GFP-CLASP$^{Mast/Orbit}$ (wild type [WT] and TOG mutant) followed by Coomassie staining. Molecular size markers (thyroglobulin, ferritin, catalase, aldolase, and BSA) were run to estimate the Stokes radius. (C) Kymographs showing MT polymerization and depolymerization with pig or S2 tubulin. Bars: (horizontal) 5 µm; (vertical) 1 min. (D) Parameters of MT polymerization dynamics in the presence of 15 µM S2 or pig tubulin alone. The mean values of each experiment are marked in gray, whereas the mean values of all the experiments are indicated by black columns (three independent experiments). Actual values are plotted in these graphs. Pausing and rescue were rarely observed in either condition. (E) Kymograph showing that kinesin-13^{Klp10A} depolymerizes MT seeds. 100 nM kinesin-13^{Klp10A} was mixed with GMPCPP-MT seeds and 10 µM Taxol. Bars: (horizontal) 5 µm; (vertical) 1 min. (F) Kymographs showing EB1-dependent tip accumulation of GFP-CLASP$^{Mast/Orbit}$. 400 nM EB1 and 100 nM CLASP$^{Mast/Orbit}$ were mixed with 30 µM pig tubulin. Bars: (horizontal) 5 µm; (vertical) 1 min. (G) Comparison of the MT growth rate in the presence or absence of EB1 (two independent experiments). Catastrophe was almost completely suppressed in either condition. (H) CLASP$^{Mast/Orbit}$ does not recruit Sentin to the MT lattice. TagRFP-CLASP$^{Mast/Orbit}$ (45 nM) was mixed with GFP-Sentin (10 nM) and MT seeds. Although TagRFP-CLASP$^{Mast/Orbit}$ localized to the MT lattice, as expected, GFP-Sentin signals were invisible. An unrelated MT-associated protein (kinesin-1 rigor mutant [560 aa]; Rice et al., 1999) and XMAP215^{Msps}, which directly binds to Sentin (Li et al., 2012), were used as negative and positive controls, respectively (each 100 nM). Bar, 20 µm.

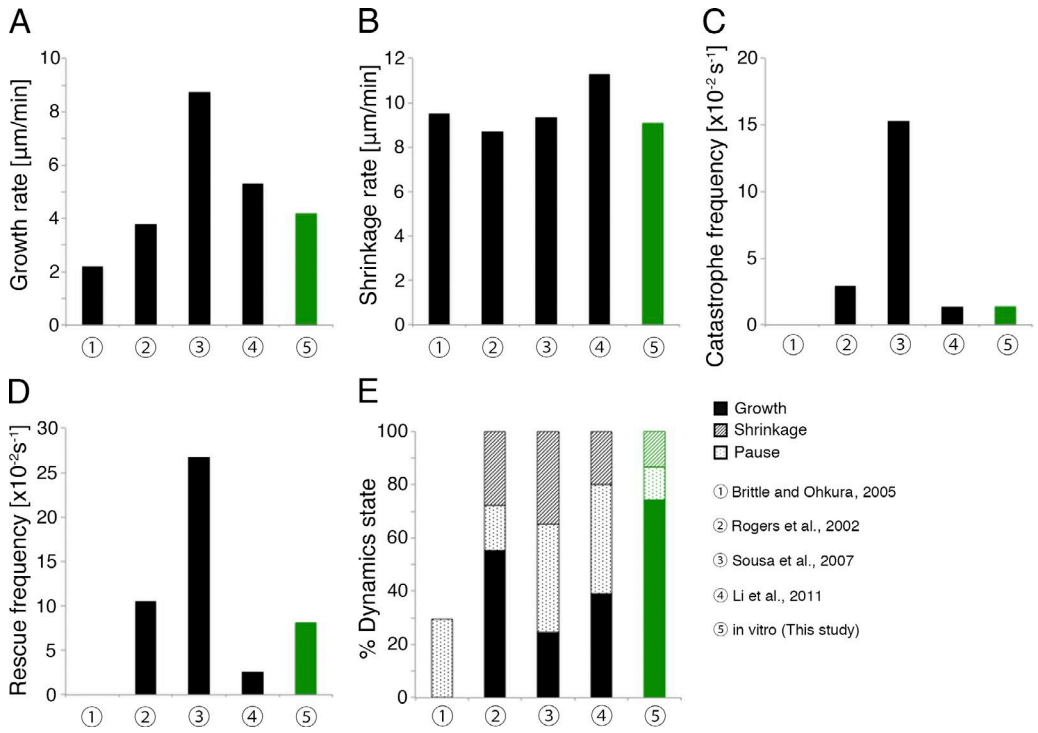

Figure S2. **Comparison of in vitro and in vivo parameters associated with MT dynamics.** Kinetic parameters of S2 interphase cytoplasmic MT dynamics presented in the previous four studies and our current in vitro study (data from Fig. 2; 15 nM CLASP$^{Mast/Orbit}$). Note that catastrophe or rescue frequency was obtained by dividing event numbers by total time in the in vivo studies. We recalculated this parameter based on the formula used in this study; event numbers were divided by total growth and pause or shrinkage time. 1, Brittle and Ohkura, 2005; 2, Rogers et al., 2002; 3, Sousa et al., 2007; 4, Li et al., 2011; 5, in vitro (this study).

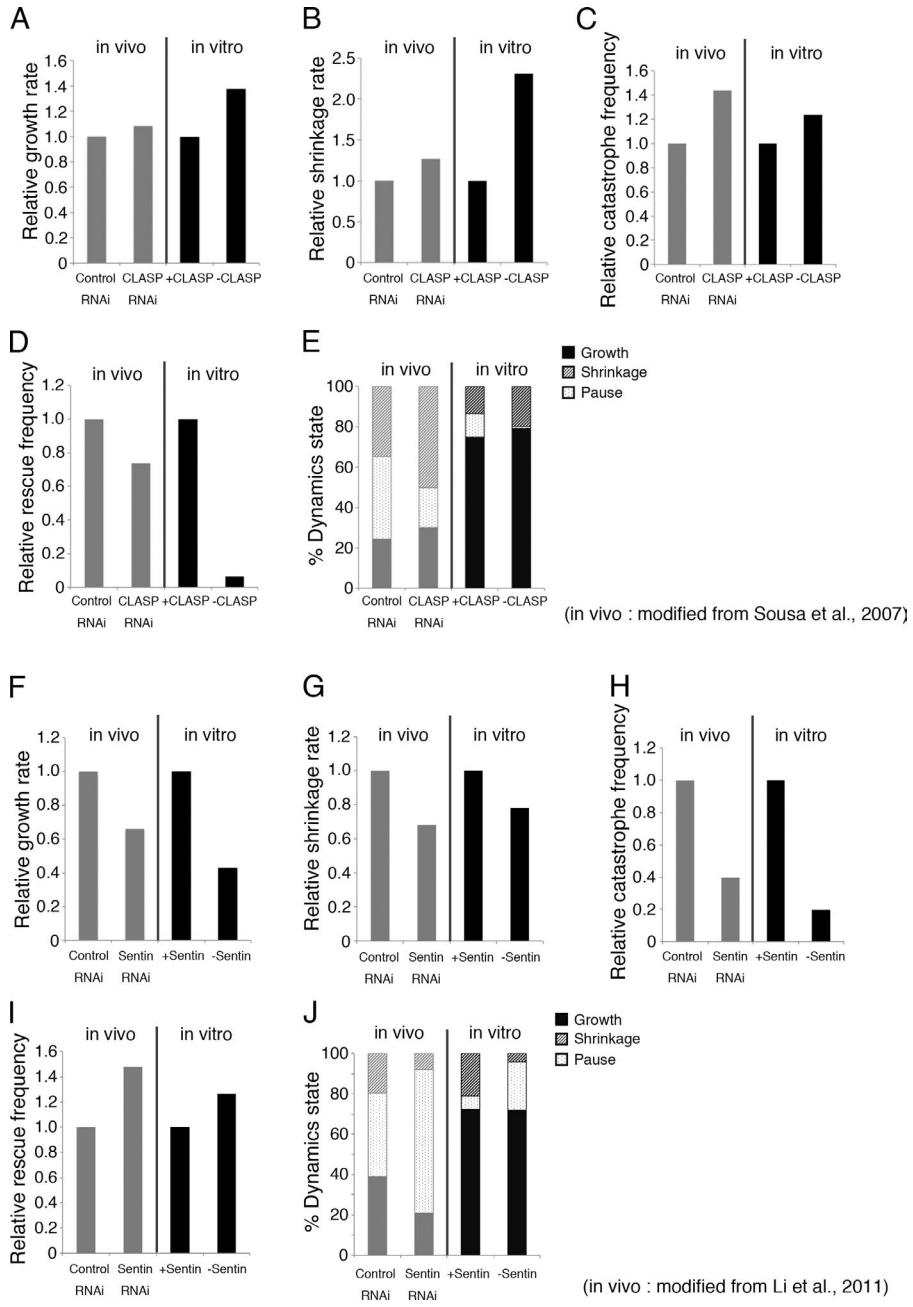

Figure S3. **Comparison of the in vitro and in vivo effects of CLASP$^{Mast/Orbit}$ and Sentin.** (A–E) Comparison of the change in kinetic parameters obtained in vivo (control vs. CLASP$^{Mast/Orbit}$ RNAi [72 h]; Sousa et al., 2007) and in vitro (five factors vs. CLASP$^{Mast/Orbit}$-depleted four factors). (F–J) Comparison of the change in kinetic parameters obtained in vivo (control vs. Sentin RNAi; Li et al., 2011) and in vitro (five factors vs. Sentin-depleted four factors). Note that catastrophe or rescue frequency was obtained by dividing event numbers by total time in the in vivo studies. We recalculated this parameter based on the formula used in this study; event numbers were divided by total growth and pause or shrinkage time.

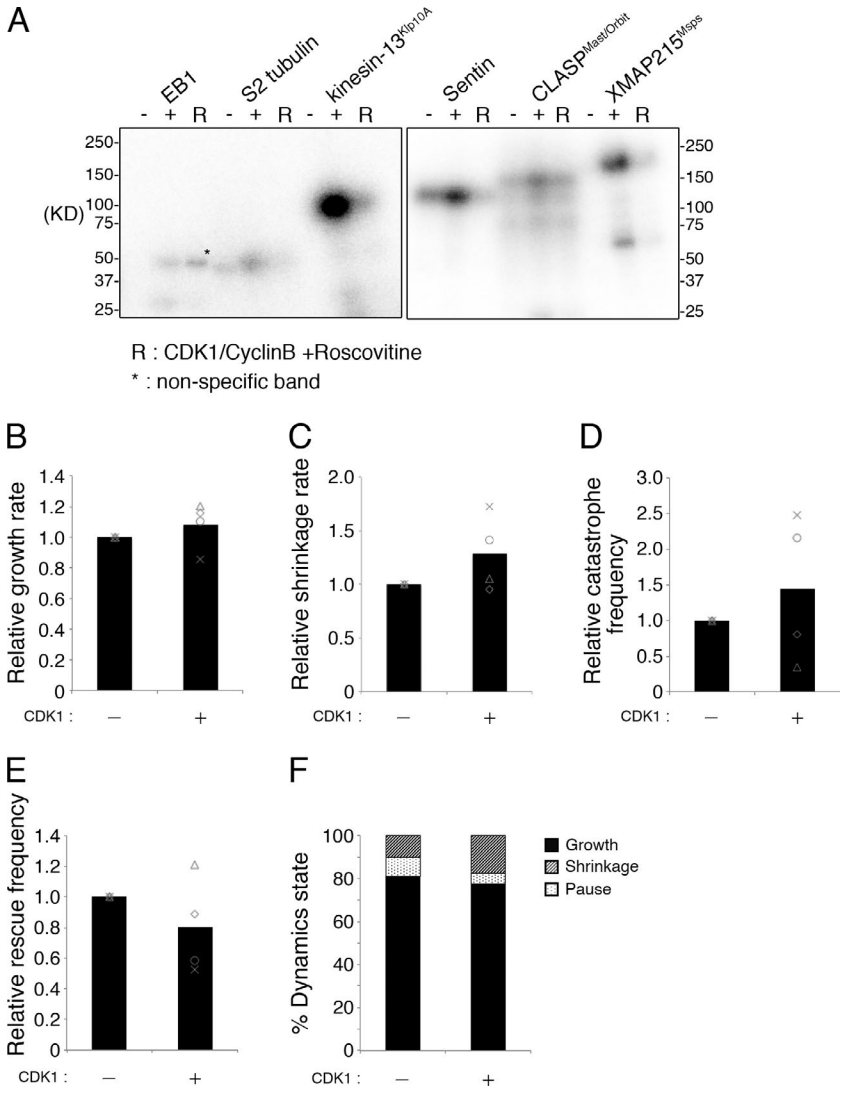

Figure S4. **Effect of Cdk1–cyclin B in MT dynamics in vitro.** (A) Autoradiography indicated that the Cdk1–cyclin B complex efficiently phosphorylates XMAP215^{Msps} and kinesin-13^{Klp10A} (4.4- and 16-fold increases in band intensity, respectively). Asterisk indicates phosphorylation of an unknown protein that represents contamination after EB1 purification (EB1 is an ∼30-kD protein [Fig. S1 A]). (B–F) Effect of Cdk1–cyclin B in MT dynamics reconstituted with five factors. Parameters of MT polymerization dynamics with 15 (cross) or 10 µM (others) S2 tubulin, XMAP215^{Msps}, EB1, Sentin, 15 nM CLASP$^{Mast/Orbit}$, kinesin-13^{Klp10A}, and 5 nM Cdk1–cyclin B (three [–] or four [+] independent experiments). Relative values are presented in this figure, whereas the actual values are described in Table S2. The mean values of each experiment are marked in gray, whereas the mean values of all the experiments are indicated by black columns. In all four experiments, the "Cdk–" condition was created by adding 50 µM roscovitine (Cdk1 inhibitor) simultaneously with recombinant Cdk1 (inhibition of the kinase activity at this roscovitine concentration had been confirmed). In two experiments (marked by a cross and triangle), the Cdk+ condition was created by DMSO addition instead of roscovitine. In other two experiments (marked by a circle and diamond), the Cdk+ condition was created by first incubating the protein mixture with Cdk1 for 15 min, followed by roscovitine addition. Note that MTs were more prone to polymerization in this experiment, because glycerol concentration in the assay buffer was higher (Cdk1 was stored in the buffer containing glycerol). Therefore, catastrophe was a rare event compared with other experiments; the difference in catastrophe frequency in the presence or absence of roscovitine should therefore be interpreted with caution.

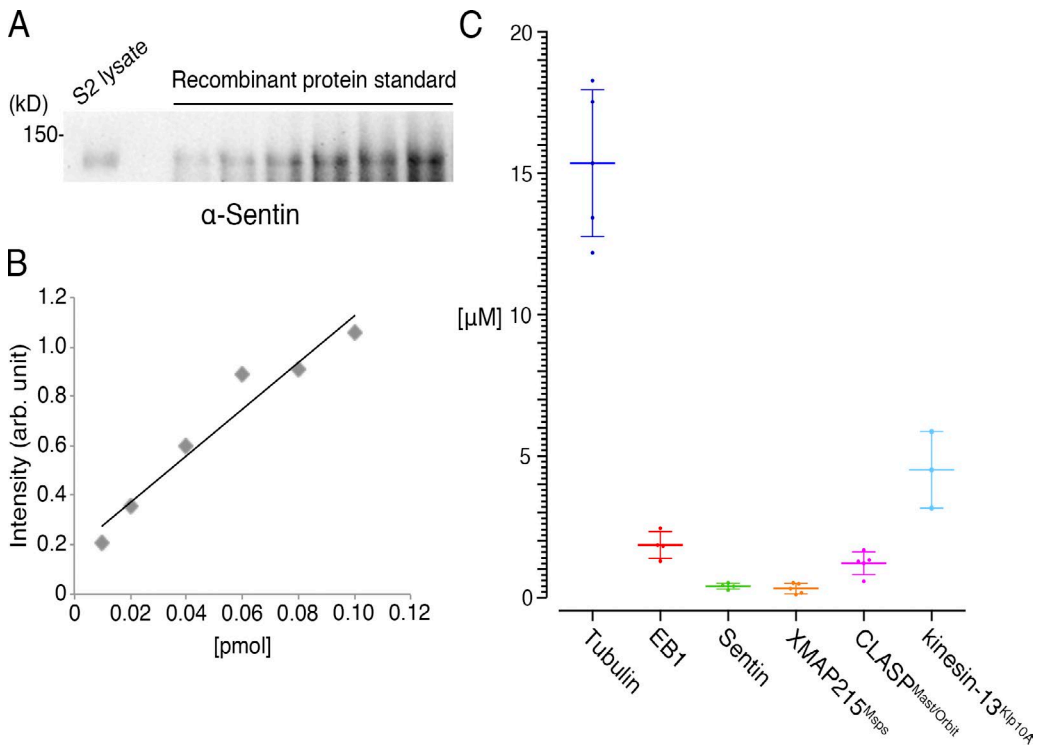

Figure S5. **Estimate of cellular protein concentration.** (A and B) An example of quantitative immunoblotting. In this case, the total cell lysate of 2×10^4 S2 cells and 5–50 fmol recombinant His-Sentin was loaded and immunoblotting was performed with an anti-Sentin polyclonal antibody. Intensity of each band corresponding to Sentin protein was measured and plotted. (C) Rough estimates of cellular protein concentration using the approximate volume of the S2 cytoplasm (spherical nuclear volume [7.5 μm diameter] was subtracted from spherical S2 cell volume [11.8 μm diameter]). Experiments were performed two to three times, and immunoblotting and band intensity measurements were duplicated (each point in the graph shows a result of each measurement). Mean and SD values are presented. The number of measurements are five (tubulin), four (EB1), four (Sentin), five (XMAP215^{Msps}), five (CLASP$^{Mast/Orbit}$), and three (kinesin-13^{Klp10A}).

Table S1. **Kinetic parameters of in vitro–reconstituted MT polymerization dynamics with or without Sentin**

Condition	*n*	Growth rate	Shrinkage rate	Catastrophe frequency	Rescue frequency
		μm/min	*μm/min*	*×10⁻³ s⁻¹*	*×10⁻³ s⁻¹*
With Sentin	3	4.7 ± 0.8 (283)	8.0 ± 1.7 (239)	24.0 ± 10.2 (227)	85.7 ± 32.9 (232)
Without Sentin	3	2.0 ± 0.4 (179)	6.1 ± 1.5 (92)	4.4 ± 2.3 (85)	95.0 ± 26.1 (86)
P		0.006 (*n* = 3)	0.227 (*n* = 3)	0.032 (*n* = 3)	0.719 (*n* = 3)
		$<10^{-4}$ (exp1) $<10^{-4}$ (exp2) $<10^{-4}$ (exp3)	0.062 (exp1) 0.001 (exp2) 0.040 (exp3)		

Values are mean ± SD of three independent experiments (total number of events). See Fig. 3 for a graphic presentation of these results.

Table S2. **Kinetic parameters of in vitro–reconstituted MT polymerization dynamics with or without Cdk1**

Condition	*n*	Growth rate	Shrinkage rate	Catastrophe frequency	Rescue frequency
		μm/min	*μm/min*	*×10⁻³ s⁻¹*	*×10⁻³ s⁻¹*
With Cdk1	3	4.7 ± 2.0 (181)	4.9 ± 0.7 (135)	9.7 ± 4.6 (120)	74.8 ± 18.4 (135)
Without Cdk1	4	5.0 ± 1.8 (251)	6.2 ± 1.1 (184)	12.4 ± 6.9 (161)	57.8 ± 17.6 (184)
P		0.73 (*n* = 3, 4)	0.13 (*n* = 3, 4)	0.63 (*n* = 3, 4)	0.38 (*n* = 3, 4)
		$<10^{-4}$ (exp1) 0.085[a] (exp2) 0.011 (exp3) 0.102 (exp4)	0.307[b] (exp1) 0.007 (exp2) 0.625 (exp3) 0.001 (exp4)		

Values are mean ± SD of three independent experiments (total number of events). See Fig. S4 for a graphic presentation of these results.
[a]In this experiment, the growth rate was decreased by Cdk1 treatment.

[b]In this experiment, the shrinkage rate was decreased by Cdk1 treatment.

Table S3. **Kinetic parameters of in vitro–reconstituted MT polymerization dynamics with or without Plk1^{Polo}**

Condition	*n*	Growth rate	Shrinkage rate	Catastrophe frequency	Rescue frequency
		μm/min	*μm/min*	*×10^{-3} s^{-1}*	*×10^{-3} s^{-1}*
Without Polo	3	3.1 ± 0.2 (314)	5.5 ± 0.1 (289)	19.6 ± 5.9 (241)	45.8 ± 9.3 (290)
With Polo	3	4.2 ± 0.5 (191)	6.7 ± 0.6 (190)	36.0 ± 8.0 (86)	27.1 ± 15.5 (186)
P		0.032 (*n* = 3)	0.027 (*n* = 3)	0.046 (*n* = 3)	0.147 (*n* = 3)
		0.001 (exp1) <10^{-4} (exp2) 0.093 (exp3)	0.016 (exp1) 0.002 (exp2) 0.127 (exp3)		

Values are mean ± of three independent experiments (total number of events). See Fig. 5 for a graphic presentation of these results.

References

Brittle, A.L., and H. Ohkura. 2005. Mini spindles, the XMAP215 homologue, suppresses pausing of interphase microtubules in *Drosophila*. *EMBO J.* 24:1387–1396. http://dx.doi.org/10.1038/sj.emboj.7600629

Li, W., T. Miki, T. Watanabe, M. Kakeno, I. Sugiyama, K. Kaibuchi, and G. Goshima. 2011. EB1 promotes microtubule dynamics by recruiting Sentin in *Drosophila* cells. *J. Cell Biol.* 193:973–983. http://dx.doi.org/10.1083/jcb.201101108

Li, W., T. Moriwaki, T. Tani, T. Watanabe, K. Kaibuchi, and G. Goshima. 2012. Reconstitution of dynamic microtubules with *Drosophila* XMAP215, EB1, and Sentin. *J. Cell Biol.* 199:849–862. http://dx.doi.org/10.1083/jcb.201206101

Rice, S., A.W. Lin, D. Safer, C.L. Hart, N. Naber, B.O. Carragher, S.M. Cain, E. Pechatnikova, E.M. Wilson-Kubalek, M. Whittaker, et al. 1999. A structural change in the kinesin motor protein that drives motility. *Nature.* 402:778–784. http://dx.doi.org/10.1038/45483

Rogers, S.L., G.C. Rogers, D.J. Sharp, and R.D. Vale. 2002. *Drosophila* EB1 is important for proper assembly, dynamics, and positioning of the mitotic spindle. *J. Cell Biol.* 158:873–884. http://dx.doi.org/10.1083/jcb.200202032

Sousa, A., R. Reis, P. Sampaio, and C.E. Sunkel. 2007. The *Drosophila* CLASP homologue, Mast/Orbit regulates the dynamic behaviour of interphase microtubules by promoting the pause state. *Cell Motil. Cytoskeleton.* 64:605–620. http://dx.doi.org/10.1002/cm.20208